Calmodulin Mediates Ca^{2+}-dependent Modulation of M-type K^+ Channels

Nikita Gamper and Mark S. Shapiro

Department of Physiology, University of Texas Health Science Center at San Antonio, San Antonio, TX 78229

ABSTRACT To quantify the modulation of KCNQ2/3 current by $[Ca^{2+}]_i$ and to test if calmodulin (CaM) mediates this action, simultaneous whole-cell recording and Ca^{2+} imaging was performed on CHO cells expressing KCNQ2/3 channels, either alone, or together with wild-type (wt) CaM, or dominant-negative (DN) CaM. We varied $[Ca^{2+}]_i$ from <10 to >400 nM with ionomycin (5 μM) added to either a 2 mM Ca^{2+}, or EGTA-buffered Ca^{2+}-free, solution. Coexpression of wt CaM made KCNQ2/3 currents highly sensitive to $[Ca^{2+}]_i$ (IC_{50} 70 ± 20 nM, max inhibition 73%, $n = 10$). However, coexpression of DN CaM rendered KCNQ2/3 currents largely $[Ca^{2+}]_i$ insensitive (max inhibition 8 ± 3%, $n = 10$). In cells without cotransfected CaM, the Ca^{2+} sensitivity was variable but generally weak. $[Ca^{2+}]_i$ modulation of M current in superior cervical ganglion (SCG) neurons followed the same pattern as in CHO cells expressed with KCNQ2/3 and wt CaM, suggesting that endogenous M current is also highly sensitive to $[Ca^{2+}]_i$. Coimmunoprecipitations showed binding of CaM to KCNQ2–5 that was similar in the presence of 5 mM Ca^{2+} or 5 mM EGTA. Gel-shift analyses suggested Ca^{2+}-dependent CaM binding to an "IQ-like" motif present in the carboxy terminus of KCNQ2–5. We tested whether bradykinin modulation of M current in SCG neurons uses CaM. Wt or DN CaM was exogenously expressed in SCG cells using pseudovirions or the biolistic "gene gun." Using both methods, expression of both wt CaM and DN CaM strongly reduced bradykinin inhibition of M current, but for all groups muscarinic inhibition was unaffected. Cells expressed with wt CaM had strongly reduced tonic current amplitudes as well. We observed similar $[Ca^{2+}]_i$ rises by bradykinin in all the groups of cells, indicating that CaM did not affect Ca^{2+} release from stores. We conclude that M-type currents are highly sensitive to $[Ca^{2+}]_i$ and that calmodulin acts as their Ca^{2+} sensor.

KEY WORDS: potassium channel • calcium • bradykinin • sympathetic neuron • M current

INTRODUCTION

M current is a voltage-gated, noninactivating K^+ current (Brown and Adams, 1980; Constanti and Brown, 1981) present in many neurons that plays a strong role in determining neuronal excitability (Jones et al., 1995; Wang and McKinnon, 1995). It has been identified as resulting from the heteromeric assembly of KCNQ2, KCNQ3 (Wang et al., 1998; Roche et al., 2002), and KCNQ5 (Lerche et al., 2000; Schroeder et al., 2000) subunits. Modulation of cloned KCNQ2/3 channels by cloned M_1 receptors has all the characteristics of muscarinic modulation of native M current in mammalian sympathetic neurons (Selyanko et al., 2000; Shapiro et al., 2000). In those neurons, several distinct second messenger–mediated signaling pathways modulate it strongly. One signal is initiated by the M_1 subtype of muscarinic acetylcholine (mAch) (Bernheim et al., 1992; Hamilton et al., 1997) or angiotensin II AT_1 (Shapiro et al., 1994) receptors via G proteins of the $G_{q/11}$ class (Delmas et al., 1998; Haley et al., 1998) and a diffusible messenger (Selyanko et al., 1992) that is not Ca^{2+} and may be a phosphoinositide (Suh and Hille, 2002; Zhang et al., 2003). Another signal provoked by bradykinin B_2 and purinergic P_{2Y} receptors involves rises in Ca^{2+}, and uses the traditional phospholipase C/inositol triphosphate (PLC/IP_3) pathway and release of Ca^{2+} from internal stores (Jones et al., 1995; Cruzblanca et al., 1998; Bofill-Cardona et al., 2000; Delmas et al., 2002; Scholze et al., 2002). Specificity in these two $G_{q/11}$-mediated signals may arise from their organization in distinct membrane microdomains (Delmas et al., 2002).

Previous work suggests that intracellular Ca^{2+} ($[Ca^{2+}]_i$) itself modulates M current, but the data concerning Ca^{2+}-mediated M current regulation are conflicting. Whereas M channels in mammalian sympathetic neurons were shown to be inhibited by $[Ca^{2+}]_i$ with an IC_{50} of 100 nM (Selyanko and Brown, 1996a,b), M current in amphibian neurons has been shown to display a more complex Ca^{2+} sensitivity (Marrion et al., 1991; Tokimasa, 1996; Tokimasa et al., 1996, 1997; Yu et al., 1994). Furthermore, it has not been determined if any such action of Ca^{2+} is direct, or if some Ca^{2+}-sensing protein is involved. Inhibition of mammalian M current by intracellular Ca^{2+} has seemed consistent with the involvement of the PLC/IP_3 cascade in bradykinin modulation of M current in sympathetic neurons,

Address correspondence to Mark S. Shapiro, Department of Physiology, MS 7756, University of Texas Health Science Center at San Antonio, 7703 Floyd Curl Drive, San Antonio, TX 78229. Fax: (210) 567-4410; E-mail: shapirom@uthscsa.edu

although the magnitude of globally measured $[Ca^{2+}]_i$ signals arising from B_2 receptor stimulation in those cells has always seemed unexpectedly modest (Cruzblanca et al., 1998; Delmas et al., 2002). In this hypothesis, the M channel is highly sensitive to $[Ca^{2+}]_i$, with raised $[Ca^{2+}]_i$ suppressing M current amplitude, and so bradykinin signaling culminates with an interaction of Ca^{2+} in some manner with the channels.

Calmodulin (CaM)* is probably the best known of an expanding class of intracellular signaling proteins that use the binding of Ca^{2+} as a molecular switch (Haeseleer et al., 2002). The protein was first characterized as the Ca^{2+} sensor for the families of Ca^{2+}/CaM-dependent protein kinases that are found in nearly every eukaryotic organism and mediate a vast array of Ca^{2+}-dependent intracellular responses. However, much recent work has revealed CaM to act as the Ca^{2+} sensor of several types of ion channels that are modulated by Ca^{2+} via mechanisms distinct from those involving kinases or phosphatases (Saimi and Kung, 2002). In some of these cases, such as high-threshold Ca^{2+} channels, CaM actions involve binding to a motif on the channels, usually called an "IQ domain," that is so named because it often contains an isoleucine and a glutamine (Lee et al., 1999; Peterson et al., 1999; Qin et al., 1999; Zuhlke et al., 1999). For several other ion channels, CaM acts by interacting with amphiphilic α (Baa) "1–5–10" or "1–8–14" domains (Chen and Yau, 1994; Ehlers et al., 1996; Schonherr et al., 2000; Trudeau and Zagotta, 2002), or in the case of small-conductance Ca^{2+}-activated K^+ (SK) channels, with novel CaM-binding domains (Xia et al., 1998; Keen et al., 1999). Sequence analysis reveals motifs with aspects of IQ-like, as well as 1–5–10-like, domains on all five KCNQ channel subtypes (Yus-Najera et al., 2002).

With the ability to reconstitute M current in a heterologous system with a low background, we saw the opportunity to firmly establish the relationship between $[Ca^{2+}]_i$ and M-type channels and to ask if indeed rises in $[Ca^{2+}]_i$ in the appropriate physiological range depress M current. Thus, we quantified the relationship between $[Ca^{2+}]_i$ and M current in intact cells using cloned KCNQ2/3 channels heterologously expressed in cells with very little endogenous K^+ current, and to determine if calmodulin mediates the action. By varying $[Ca^{2+}]_i$ without concomitant G protein activation and the use of active or dominant-negative calmodulin, we show that calmodulin confers a high sensitivity of KCNQ2/3 channels to $[Ca^{2+}]_i$, in the range shown by Selyanko and Brown (1996a) for M channels in inside-out patches from neurons. We also tested the hypothesis that bradykinin-induced rises of Ca^{2+} acts on M channels via Ca^{2+}/CaM. We indeed find evidence that CaM mediates $[Ca^{2+}]_i$ modulation of M-type channels and that bradykinin modulation involves actions in concert with CaM, whereas muscarinic acetylcholine receptor (mAchR)-mediated modulation is Ca^{2+}/CaM-independent.

Abbreviations used in this paper: CaM, calmodulin; CHO, Chinese hamster ovary; DN, dominant-negative calmodulin; EGFP, enhanced green fluorescent protein; mAchR, muscarinic acetylcholine receptor; SCG, superior cervical ganglion.

MATERIALS AND METHODS

cDNA Constructs

Plasmids encoding human KCNQ2, rat KCNQ3, human KCNQ4, and human KCNQ5 (Genbank accessions AF110020, AF091247, AF105202, and AF249278, respectively) were given to us by David McKinnon (KCNQ2, KCNQ3; SUNY, Stony Brook, N.Y.), Thomas Jentsch (KCNQ4; Zentrum fur Molekulare Neurobiologie, Hamburg, Germany), and Klaus Steinmeyer (KCNQ5; Aventis Pharma, Frankfurt am Main, Germany). Plasmids containing wild-type (wt) (Persechini et al., 1989) or dominant-negative (DN) vertebrate CaM were given to us by Trisha Davis (University of Washington, Seattle, WA). DN CaM has an alanine substitution in each of the four Ca^{2+}-binding EF hands (D20A, D56A, D93A, D129A). The wt and DN CaM coding regions were subcloned by PCR into the pcDNA3 mammalian expression vector (Invitrogen) using BamH1 and Xba1. KCNQ2 and KCNQ3 were subcloned into pcDNA3 as described previously (Shapiro et al., 2000). Myc-tagged KCNQ2–5 were generated by subcloning each channel in frame into pCMV-myc (CLONTECH Laboratories, Inc.) behind the myc epitope.

Cell Culture and Transfections

Chinese hamster ovary (CHO) cells were a gift of Feng Liu (Department of Pharmacology, UTHSCSA, San Antonio, TX). Cells were grown in 100-mm tissue culture dishes (Falcon) in DMEM medium with 10% heat-inactivated fetal bovine serum plus 0.1% penicillin/streptomycin in a humidified incubator at 37°C (5% CO_2) and passaged about every 4 d. Cells were discarded after ~30 passages. For transfection, cells were plated onto poly-L-lysine coated coverslip chips, transfected 24 h later with Polyfect reagent (QIAGEN) according to the manufacturer's instructions, and experiments were performed 48–96 h after transfection. As a marker for successfully transfected cells, cDNA-encoding green fluorescent protein (GFP) was cotransfected together with the cDNAs of the genes of interest. We found that >95% of green-fluorescing cells express KCNQ2/3 currents in control experiments.

SCG Neuron Culture and Transduction/Transfection

Sympathetic neurons were isolated from the superior cervical ganglia (SCG) of 3–14-d-old male rats (Sprague-Dawley) and cultured for 2–4 d. Rats were anesthetized with halothane and decapitated. Neurons were dissociated using methods of Bernheim et al. (1991), plated on 4 × 4 mm glass coverslips (coated with poly-L-lysine) and incubated at 37°C (5% CO_2). Fresh culture medium containing nerve growth factor (50 ng/ml) was added to the cells 3 h after plating. For exogenous expression of wt and DN CaM in SCG neurons, we used two expression methods. The first was the Sindbis α-viral system, and the second was the biolistic particle delivery system ("gene gun"; Bio-Rad Laboratories).

To construct the appropriate plasmids for the Sinbis method (Invitrogen), wt or DN CaM cDNA was subcloned by PCR into the multiple cloning site of pIRES2-EGFP (CLONTECH Labora-

tories, Inc.) using Sal1 and Xma1, and nonmethylated DNA extracted from SCS110 *E. coli* (Stratagene). The CaM-IRES-EGFP coding regions flanked by Xba1-Xba1 were then subcloned into the pSinRep5 vector (Invitrogen) using Nhe1. Proper directional cloning was verified with a BamHI digest. Pseudovirions were generated in baby hamster kidney cells according to the Sindbis manual using in vitro RNA transcripts (mMessage mMachine; Ambion) of the constructed plasmids just described and DH(26S) helper plasmid. Infection of cells with these pseudovirions leads to expression of wt or DN CaM and EGFP as separate proteins from a common promoter, allowing us to identify transduced cells with EGFP fluorescence. Recordings from transduced cells were made between 12 and 18 h after exposure to pseudovirions.

For the biolistic method, we used the PDS-1000/He gene gun (Bio-Rad Laboratories) according to the manufacturer's instructions. In brief, cDNA subcloned into the bicistronic pIRES2 vector was coated onto 1-μm gold particles, spread on to the supplied macrocarriers in an ethanolic solution, and allowed to dry in a dessicated environment. We used a burst pressure of 650 psi, which we empirically found to give the optimal expression efficiency in SCG neurons. Cells were plated onto glass coverslips at the time of dissociation, cultured overnight in 35-mm dishes, and "shot" in those same dishes, with the cells already adhered to the coverslips that we used for experiments. The culture medium was aspirated from the dishes, bombardment performed at the topmost slot in the bombardment chamber under 15–17 inches Hg of vacuum, and fresh culture medium immediately added to the dishes. Transfection efficiency was assumed to occur by the random distribution of fired gold particles, and was ~5% of cultured neurons.

Electrophysiology

The whole-cell configuration of the patch-clamp technique was mostly used to voltage clamp and dialyze cells at room temperature (22–25°C). Pipettes were pulled from borosilicate glass capillaries (1B150F-4; World Precision Instruments) using a Flaming/Brown micropipette puller P-97 (Sutter Instruments Co.) and had resistances of 2–3 MΩ when filled with internal solution and measured in standard bath solution. Membrane current was measured with pipette and membrane capacitance cancellation, sampled at 5 ms and filtered at 200 Hz by an EPC-9 amplifier and PULSE software (HEKA/Instrutech). The whole-cell access resistance was typically 4–10 MΩ. In some experiments on SCG cells, the perforated-patch method of recording was used with amphotericin B (120 ng/ml) in the pipette (Rae et al., 1991). Amphotericin was prepared as a stock solution in 60 mg/ml in DMSO. Pipette tips were very briefly dipped in pipette solution not containing amphotericin, and back-filled with amphotericin-containing solution. In these experiments, the access resistance was typically 10–20 MΩ 5–15 min after seal formation. Cells were placed in a 500-μl perfusion chamber through which solution flowed at 1–2 ml/min. Inflow to the chamber was by gravity from several reservoirs, selectable by activation of solenoid valves (ValveLink 8; Automate Scientific). Bath solution exchange was complete by <30 s.

To evaluate the amplitude of KCNQ2/3 currents, CHO cells were held at 0 mV and 500-ms hyperpolarizing steps to −60 mV, followed by a 650-ms pulse back to 0 mV, were applied every 3 s. The amplitude of the current in CHO cells was usually defined as the outward current at the holding potential sensitive to XE991 or linopirdine (50 μM), selective blockers of KCNQ channels (Zaczek et al., 1998). Cells exhibited variable "run-down" in the amplitude of KCNQ currents, and usually stabilized within several minutes of whole-cell dialysis. Cells in which the "run-down" exceeded 3% per minute were discarded. M currents in SCG cells were studied by holding the membrane potential at −25 mV and applying a 500-ms hyperpolarizing pulse to −60 mV every 3 s. M-current amplitude was measured at −60 mV from the decaying time course of the XE991/linopirdine-sensitive deactivating current as the difference between the average of a 10-ms segment, taken 20–30 ms into the hyperpolarizing step and the average during the last 50 ms of that step. All results are reported as mean ± SEM.

Ca^{2+} Imaging

For simultaneous patch-clamp recording and Ca^{2+} imaging of CHO and SCG cells, we pipette-loaded fura-2 (100 μM) as the pentapotassium salt. After gigaseal formation, single images at 340 and 380 nm were acquired for background correction. After dialysis for 5–10 min, the imaging protocol was triggered in synchrony by the PULSE software. Fluorescent microscopy was performed with an inverted Nikon Eclipse TE300 microscope in DIC configuration with an oil-immersion 40×/1.30 NA objective. A Polychrome IV monochromator (T.I.L.L. Photonics) was used as the excitation light source and FURA2 71000 and FITC HQ 96170M filter cubes (Chroma) were used for fura-2 and GFP imaging, respectively. Cells were excited alternatively at 340 and 380 nm (50–200 ms every 2s) and the fluorescence emission collected by an IMAGO 12-bit cooled CCD camera and images stored/analyzed with TILLvisION 4.0 software. Ratiometric data were converted to $[Ca^{2+}]_i$ by using the equation $[Ca^{2+}]_i = K^*(R - R_{min})/(R_{max} - R)$, where R is the 340/380 nm fluorescence ratio and R_{min} and R_{max} are the ratios of Ca^{2+}-free and Ca^{2+}-bound dye, respectively (Grynkiewicz et al., 1985). R_{min}, R_{max}, and K* were measured from cells dialyzed with a KCl-based internal solution containing (in mM) 20 BAPTA, 5 $MgCl_2$ and 5 HEPES (R_{min}) or 10 $CaCl_2$, 5 $MgCl_2$ and 5 HEPES (R_{max}) or 20 BAPTA, 10 Ca^{2+}, 5 $MgCl_2$, 5 HEPES (K*), and the values calculated were 0.15, 2.16, and 1.081 μM, respectively (n = 4–5 cells for each). For the experiments assaying bradykinin-induced Ca^{2+} raises, SCG neurons were bath loaded with fura-2 AM (2 μM) for 30 min at 37°C in the presence of pluronic acid (0.01%). These fura-2 signals were not calibrated due to inherent difficulties in calibrating esterified indicator dyes (Zhou and Neher, 1993).

Gel-shift Assays

To assay for binding of CaM to IQ-like domains of KCNQ2 and KCNQ3, 0.5–5 μg of purified recombinant vertebrate CaM (given to us by Linda J. Roman and Bettie Sue Masters, Department of Biochemistry, UTHSCSA, San Antonio, TX) was incubated for 1 h at room temperature with an IQ_1 peptide of KCNQ2 (335–355, PAAGLIQSAWRFYATNLSRT), two slight variants of an IQ_1 peptide of KCNQ3 (332–354, EKRRKPAAELIQAAWRYYATNP and 337–357, PAAELIQAAWRYYATNPNRI), IQ_2 peptides of KCNQ2 or KCNQ3 (KCNQ2 508–530, SIRAVCVMRFLVSKRKFKESLR; KCNQ3 481–503, AIRAVRILQFRLYKKKFKETLR) or the IQ_L peptide (α_{1C} Ca^{2+} channel KFYATFLIQEYFRKFKKRKEQ; Peterson et al., 1999). All peptides were synthesized at the Protein Core Laboratory, UTHSCSA, San Antonio, TX. The incubations were run on nondenaturing PAGE using a 12% or 15% gel run at low voltage overnight at 4°C. Gels were either silver stained (GelCode SilverSNAP stain kit; Pierce Chemical Co.) at that point according to the instructions of the manufacturer (for which case 5 μg of CaM was run on the gel), or they were transferred to nitrocellulose and immunoblotted as described below (in which case 0.5 μg of CaM was used). The incubations and immunoblots were performed either in the presence of 2 mM Ca^{2+} or with no added Ca^{2+} plus 2 mM EGTA.

Immunoprecipitations and Immunoblotting

Cells were grown in 100-mm culture dishes and transfected with myc-tagged KCNQ2–5 and GFP, alone or together with wt or DN CaM. After 48 h, cells were harvested with a rubber policeman in RIPA lysis buffer (10 mM $NaPO_4$, 150 mM NaCl, 1% Na deoxycholate, 1% Triton X-100, 0.1% SDS) plus a cocktail of protease inhibitors (1 μM Nα-p-tosyl-L-lysine chloro-methyl ketone, 1 μM N-tosyl-L-phenylalanine chloromethyl ketone, 1 μM 4-(2-amino ethyl)-benzene sulfonyl fluoride HCl, 1 μM E-64, 1 μg/ml leupeptin and 1 μM pepstatin, all from Sigma-Aldrich) and lysate proteins quantified with a BCA assay (Pierce Chemical Co.). Proteins (400 μg/reaction) were immunoprecipitated overnight at 4°C using 2 μg of rabbit anti-CaM or anti-FAK antibodies (Santa Cruz Biotechnology, Inc.) and 40 μl of protein A/G beads (Santa Cruz Biotechnology, Inc.). Immunoprecipitated proteins bound to pelleted protein A/G beads were washed thoroughly in RIPA buffer (sometimes containing added Ca^{2+} or EGTA), denatured in Laemmli sample buffer, separated using SDS/PAGE, and electroblotted onto nitrocellulose membranes. Nonimmunoprecipitated lysates were denatured in Laemmli sample buffer, separated using SDS/PAGE, and electroblotted onto nitrocellulose membranes. Immunoblots were probed with mouse anti-myc (CLONTECH Laboratories, Inc.) or anti-CaM primary antibodies (1:1,000 dilution, overnight at 4°C) in a blocking solution containing 5% nonfat dry milk (Carnation) in TBS/Tween and subsequently treated with goat anti–mouse or anti–rabbit horseradish peroxidase–conjugated secondary antibodies (1:25,000 dilution, 45 min, room temperature; Jackson ImmunoResearch Laboratories). Blots were developed with enhanced chemiluminescence (Supersignal; Pierce Chemical Co.) and exposed on X-ray film (Biomax).

Solutions and Materials

The external solution used to record KCNQ2/3 currents in CHO cells contained (mM): 160 NaCl, 2.5 KCl, 2 $CaCl_2$, 1 $MgCl_2$, 10 HEPES, (pH 7.4 with NaOH). In experiments in which we lowered $[Ca^{2+}]_i$, Ca^{2+} was omitted from the bathing solution and EGTA (10 mM) added. The regular pipette solution contained (mM): 160 KCl, 5 $MgCl_2$, 5 HEPES, 0.1 1,2-bis(2-aminophenoxy)ethane N,N,N′,N′-tetraacetic acid (BAPTA), 3 K_2ATP, 0.1 KGTP (pH 7.4 with KOH). Reagents were obtained as follows: BAPTA, fura-2, fura-2 AM, ionomycin, pluronic acid (Molecular Probes); DMEM, fetal bovine serum, nerve growth factor, penicillin/streptomycin (GIBCO BRL); ATP and GTP, (Sigma-Aldrich); amphotericin B (Calbiochem) XE991 and linopirdine were gifts of Michael E. Schnee (Dupont Pharmaceuticals).

RESULTS

Tests of Sensitivity to $[Ca^{2+}]_i$ of Heterologously Expressed KCNQ2/3 Channels

We tested the Ca^{2+} sensitivity of KCNQ2/3 heteromeric channels in a heterologous expression system in which the cDNA clones for KCNQ2 and KCNQ3, as well as GFP as a reporter, were transiently transfected into chinese hamster ovary (CHO) cells. Cells cotransfected with KCNQ2 and KCNQ3 gave large currents typical of KCNQ2/3 heteromultimers with the appropriate blockade by 10 mM tetraethylammonium ions (48 ± 3%, $n = 5$) (Shapiro et al., 2000). Untransfected CHO cells display very little endogenous K^+ current, making them a suitable cell line for these studies. Simultaneous whole-cell clamp recording and Ca^{2+} imaging was performed on cells 2–4 d after transfection, with 100 μM fura-2 dialyzed into the cytoplasm via the patch pipette. We sought to vary intracellular Ca^{2+} ($[Ca^{2+}]_i$) in a way that was independent of G-protein activation (which might modulate KCNQ2/3 channels by other means) and to directly examine the effect of $[Ca^{2+}]_i$ on the KCNQ2/3 current. We accomplished this by perfusion of cells with a bathing solution containing a low concentration (5 μM) of the Ca^{2+} ionophore ionomycin and either 2 mM Ca^{2+}, ("2 Ca") or no added Ca^{2+} together with 10 mM EGTA ("0 Ca"). Using these two solutions, we were able to vary $[Ca^{2+}]_i$ in a concentration range from <10 to >400 nM, reproducibly and in a controlled manner. The vehicle for ionomycin (DMSO 0.5%) did not affect the KCNQ2/3 current. Fig. 1 A shows such an experiment in which application of ionomycin plus 2 Ca to a cell ramped $[Ca^{2+}]_i$ from ~80 nM to >300 nM within several minutes. There was little response of the KCNQ2/3 current to the change in $[Ca^{2+}]_i$, except at very high $[Ca^{2+}]_i$ where the current amplitude started to decrease. In general, we found that the sensitivity of the KCNQ2/3 current to $[Ca^{2+}]_i$, was low and rather variable from cell to cell. For a couple cells, there was evidence of more $[Ca^{2+}]_i$ sensitivity in the KCNQ2/3 current amplitude, but for most, as in the example in Fig. 1 A, the $[Ca^{2+}]_i$ sensitivity was weak, suggesting to us that the $[Ca^{2+}]_i$ sensitivity in any given cell might be dependent on the relative abundance of expressed KCNQ2/3 channels and some endogenous Ca^{2+}-sensing protein.

Calmodulin Confers Strong Ca^{2+} Sensitivity to KCNQ2/3 Channels

To test if calmodulin (CaM) might be the Ca^{2+} sensor of KCNQ2/3 channels, we examined the effects of wild-type (wt) CaM, or a dominant-negative mutant CaM (DN CaM) in which all four EF-hands have the aspartate to alanine mutation, rendering it unable to bind Ca^{2+} (Geiser et al., 1991). To confirm that our DN CaM does not bind Ca^{2+}, whole-cell lysates from CHO cells transfected with wt or DN CaM were run on Western gels in the presence of Ca^{2+} or of EGTA, and immunoblotted with anti-CaM antibodies (Fig. 1, inset). Lysate from cells expressing wt CaM, but not from those expressing DN CaM, migrated on the gel with an obvious Ca^{2+}-dependent mobility shift (we ascribe the faint component from DN CaM cells which does seem to have a shift to endogenous CaM).

We compared the Ca^{2+} sensitivity of KCNQ2/3 currents in cells cotransfected with either wt CaM or with DN CaM. Fig. 1 B shows the results from a cell transfected with wt CaM together with KCNQ2/3 channels. A protocol similar to that used in Fig. 1 A was used to

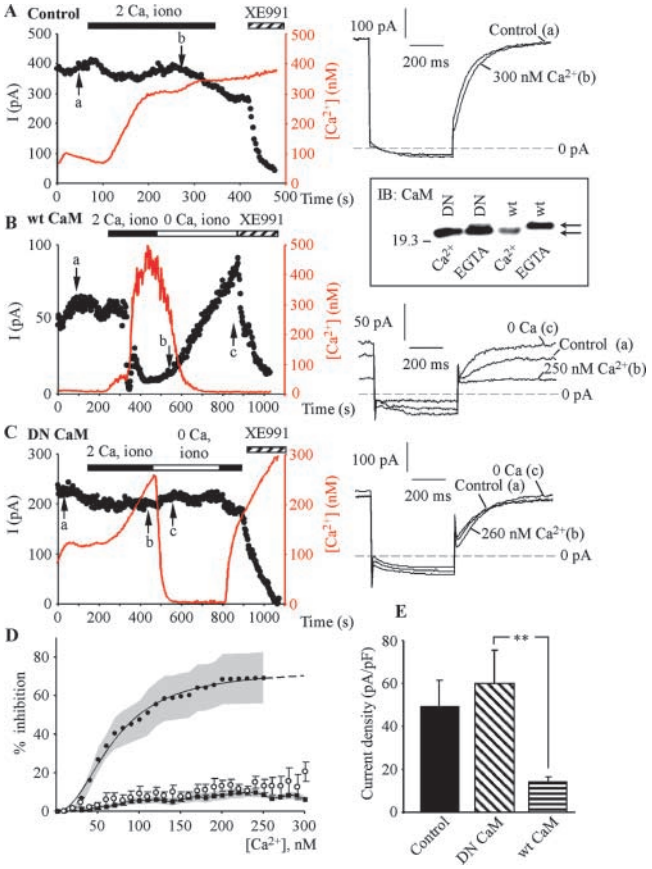

FIGURE 1. Calmodulin confers high Ca^{2+} sensitivity to KCNQ2/3 channels. CHO cells were cotransfected with KCNQ2 and KCNQ3 alone (A) or together with wt CaM (B) or DN CaM (C). KCNQ2/3 currents were recorded from pulses delivered every 3 s while $[Ca^{2+}]_i$ was simultaneously monitored from fluorescence of fura-2 (100 μM) loaded via the patch pipette. Plotted in the left panels in A–C are the current amplitudes (filled circles) and $[Ca^{2+}]_i$ (red line), calculated as described in MATERIALS AND METHODS. Bath solutions containing ionomycin (5 μM) in either the 2 mM or 0 Ca^{2+} solutions, or XE991 (50 μM) were applied during the periods indicated by the bars. Representative current traces are shown in the right-hand panels. In the inset is shown an immunoblot using an anti-CaM antibody of whole-cell lysates from CHO cells transfected with wt or DN CaM, run as Western gels in the presence of 2 mM Ca^{2+} or 1 mM EGTA. (D) The data for all experiments such as in A–C using non-CaM overexpressing ($n = 9$, open circles), wt ($n = 10$, closed circles) or DN CaM ($n = 10$, filled squares) overexpressing CHO cells were pooled and plotted as a dose-response curve of inhibition versus $[Ca^{2+}]_i$. For each experiment, the current and $[Ca^{2+}]_i$ records were temporally aligned, $[Ca^{2+}]_i$ was binned in 10 nM widths, and the current amplitudes within the appropriate time period were averaged. The current was normalized to the maximal current (I_{max}). The standard error for each bin in wt or DN CaM overexpressing cells is shown as the shaded region along the curve, and that for control cells as error bars. For wt CaM-expressing cells, the data were fitted by a Hill equation of the form $(1 - I/I_{max})*100\% = a*[Ca^{2+}]_i^n/(IC_{50}^n + [Ca^{2+}]_i^n)$, where a is the maximal current inhibition and n is the Hill coefficient with values given in the text. (E) Bars show the mean initial KCNQ2/3 current density measured at 0 mV for cells transfected only with KCNQ2+3 channels (Control, $n = 14$), or together with wt ($n = 18$) or DN CaM ($n = 17$), before application of the ionomycin-containing bath solutions. **, significance at the $P \leq 0.01$ level, Student's t test.

record KCNQ2/3 currents simultaneously while varying $[Ca^{2+}]_i$ using our ionomycin solutions. Plotted are $[Ca^{2+}]_i$ (red line) and the KCNQ2/3 current amplitude (black circles). At the start of the experiment, $[Ca^{2+}]_i$ starts off very low (<10 nM); perfusion of ionomycin in 2 Ca raises $[Ca^{2+}]_i$ to nearly 500 nM within several minutes, and then perfusion of ionomycin in 0 Ca lowers $[Ca^{2+}]_i$ again to <10 nM. As can be seen, the amplitude of the KCNQ2/3 current responded briskly to changes in $[Ca^{2+}]_i$. When $[Ca^{2+}]_i$ increased, the KCNQ2/3 current amplitude declined in parallel, and when $[Ca^{2+}]_i$ was lowered, the current recovered, in this case increasing to a level even greater than that initially. However, a very different result was obtained in CHO cells cotransfected with DN CaM instead of wt CaM. In this case, the KCNQ2/3 current proved to be nearly insensitive to $[Ca^{2+}]_i$ varied over this range. Fig. 1 C shows such an experiment. When $[Ca^{2+}]_i$ was increased from <10 to >250 nM, the KCNQ2/3 current amplitude decreased by <15%.

The responses of KCNQ2/3 currents to $[Ca^{2+}]_i$ were pooled by binning $[Ca^{2+}]_i$ in 10 nM widths from <10 to 400 nM and averaging the inhibition for each bin for all cells studied. The pooled results for wt- and DN CaM–overexpressing cells and also for cells transfected with KCNQ2/3 channels only are shown in Fig. 1 D and show a dramatic increase in Ca^{2+} sensitivity of KCNQ currents induced by wt CaM overexpression. For cells cotransfected with wt CaM, there was a strong dependence of the current amplitude on $[Ca^{2+}]_i$. The data were fit by a Hill equation with an IC_{50} of 70.0 ± 20.0 nM, a saturating inhibition of 73.2 ± 1.4%, and a Hill coefficient of 2.0 ($n = 10$). Since $[Ca^{2+}]_i$ measured globally in these experiments may not accurately reflect submembrane $[Ca^{2+}]$, the IC_{50} obtained in Fig. 1 D may be only approximate. For cells cotransfected with DN CaM or those expressing no exogenous CaM, the currents were only slightly dependent on $[Ca^{2+}]_i$. Those data could not meaningfully be fit by a Hill equation. The maximal inhibition at 200 nM Ca^{2+} in cells transfected with DN CaM was only 8.3 ± 2.5% ($n = 10$), and in those not coexpressed with CaM it was 13.1 ± 2.8% ($n = 9$). Thus, these experiments indicate that, in the presence of functional CaM, KCNQ2/3 channels are highly sensitive to $[Ca^{2+}]_i$ over the physiological range of <10 to 400 nM, and suggest that CaM confers the sensitivity to the channels. The steepness of the concentration dependence also suggests that binding of at least two Ca^{2+} ions are required for Ca^{2+}/CaM actions. Cells transfected with only KCNQ2/3 channels, but not CaM, showed a very variable response to $[Ca^{2+}]_i$, as if the relative abundance of a Ca^{2+}-sensing partner might be involved. In contrast, cells cotransfected with DN CaM displayed currents only minimally sensitive to $[Ca^{2+}]_i$, suggesting that

functional CaM is necessary for Ca^{2+} modulation of KCNQ2/3 channels.

Inhibition of KCNQ2/3 current in CHO cells overexpressing wt CaM was not accompanied by any significant changes in current activation or deactivation kinetics. Measured at low $[Ca^{2+}]_i$ (40 ± 13 nM), activation and deactivation time constants in these cells were 145 ± 14 ms and 110 ± 20 ms, respectively (n = 8), whereas when measured at elevated $[Ca^{2+}]_i$ (335 ± 137 nM) these values were 135 ± 11 ms and 115 ± 9 ms (n = 8). While we did not directly measure the voltage dependence of activation of the conductance as a function of $[Ca^{2+}]_i$, the lack of any change in activation or deactivation kinetics make a shift in voltage dependence very unlikely. This is because the voltage dependence of the activation of the conductance of voltage-gated channels is the sum effect of the rates of activation and deactivation of the channels. Thus, the modulation of KCNQ2/3 current amplitudes by Ca^{2+}/CaM that we show here is very unlikely to be due to a shift in voltage dependence, in accord with that reported recently (Wen and Levitan, 2002).

In these experiments, initial $[Ca^{2+}]_i$ in cells expressed without CaM, with DN CaM, or with wt CaM were similar (63 ± 15, 54 ± 12, 60 ± 15 nM, respectively, all n = 12). Since these values are near the IC_{50} for Ca^{2+} action in cells expressed with wt CaM, we might expect that expression of wt CaM would cause an increase of tonic CaM action at "resting" $[Ca^{2+}]_i$. If so, this predicts that initial current amplitudes (before we altered $[Ca^{2+}]_i$ with our ionomycin solutions) would be considerably smaller in cells cotransfected with wt CaM. Thus, we compared the density of the KCNQ2/3 current in the groups of cells cotransfected with wt CaM, with DN CaM, or without any CaM. We found a large difference in current density in those three groups of cells (Fig. 1 E). For cells not cotransfected with CaM, the current density was 49 ± 12 pA/pF (n = 14); for cells cotransfected with DN CaM, it was 60 ± 15 pA/pF (n = 17), and for cells cotransfected with wt CaM, it was only 14 ± 2 pA/pF (n = 18, $P \leq 0.01$). The difference in current density between control and wt CaM–overexpressing cells was not due to differences in KCNQ2/3 channel expression since immunoblot analysis of whole-cell lysates from CHO cells transfected with myc-tagged KCNQ2/3 channels and wt or DN CaM did not reveal a noticeable difference in cellular channel expression in the three groups (unpublished data), although such immunoblot analysis cannot distinguish between proteins that are assembled in the membrane as channels, and those that are not. We interpret these results as suggesting that coexpression of wt CaM causes there to be tonically more Ca^{2+}-bound CaM molecules available to interact with the channels.

SCG M Current Is Sensitive to Changes in $[Ca^{2+}]_i$

We tested if endogenous M channels in rat sympathetic SCG neurons are also sensitive to $[Ca^{2+}]_i$. As for KCNQ2/3 channels in CHO cells, we reasoned that we should be able to regulate such Ca^{2+} modulation in SCG neurons by manipulating $[Ca^{2+}]_i$ using our ionomycin-containing bath solutions. Such experiments are made complicated in SCG cells by the plethora of Ca^{2+}-gated conductances that such neurons express, including several types of Ca^{2+}-activated K currents. These Ca^{2+}-activated K current, being biophysically and pharmacologically quite different from M current (no slow deactivation, very negative threshold for activation at high $[Ca^{2+}]_i$, little XE991 or linopirdine sensitivity) nevertheless produced considerable interference to our measurements, especially at high $[Ca^{2+}]_i$. To minimize such interference, we designed a protocol that allowed short and relatively small (within 200 nM) Ca^{2+} rises (Fig. 2). In such experiments we started to perfuse cells with EGTA-buffered Ca^{2+}-free solution (without ionomycin) shortly after gigaseal formation and continued perfusion during the loading of fura-2 into the cell. Thus, we started to measure M current amplitude and fura-2 fluorescence at relatively low initial $[Ca^{2+}]_i$ (usually 30–50 nM). $[Ca^{2+}]_i$ was then elevated by a brief application of ionomycin-containing 2 mM Ca^{2+} solution. Once elevation of $[Ca^{2+}]_i$ was detected, perfusion was switched back to Ca^{2+}-free solution, preventing an exceedingly high $[Ca^{2+}]_i$ rise that could turn on Ca^{2+}-activated conductances. Fig. 2 A shows one such experiment. Elevation of $[Ca^{2+}]_i$ from ~80 to ~150 nM induced a strong suppression of M current amplitude that then recovered when $[Ca^{2+}]_i$ was lowered back to its initial level. Data from nine such experiments are summarized in Fig. 2 B. An increase of $[Ca^{2+}]_i$ from 49 ± 9 nM to 241 ± 23 nM was accompanied by a reversible decrease of M current amplitude by 47 ± 10%. Thus, native M current is also highly $[Ca^{2+}]_i$ sensitive, and the sensitivity is in a similar range of $[Ca^{2+}]_i$ as that for KCNQ2/3 channels coexpressed with wt CaM in CHO cells.

CaM Binds to KCNQ2–5 Subunits and to an IQ Domain on KCNQ3 Channels

Our physiological experiments suggested that CaM might act by interacting with the channel proteins. It has been demonstrated that neuronal M-type currents are made by various combinations of KCNQ2–5 subunit types (Jentsch, 2000; Roche et al., 2002; Shah et al., 2002). It seems that KCNQ3 can act as the "master subunit," for it coassembles with KCNQ2 and KCNQ5, but the latter two not with each other. Recent work has focused on binding of CaM to domains on KCNQ2 channels (Wen and Levitan, 2002; Yus-Najera et al.,

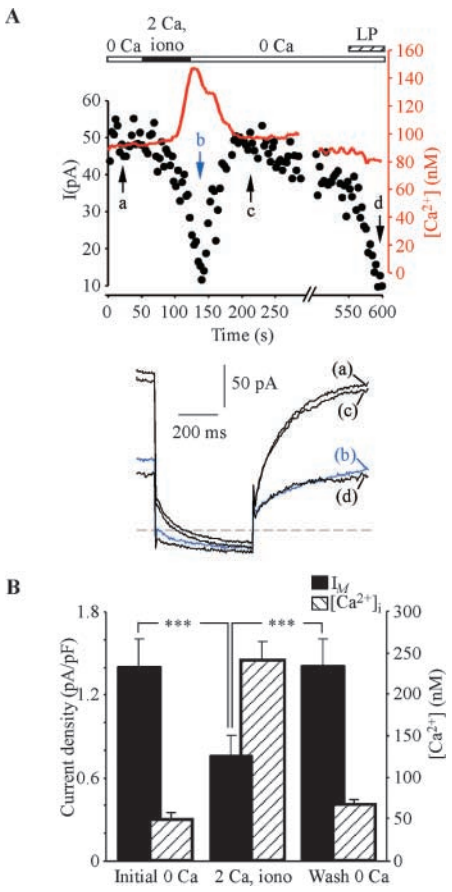

FIGURE 2. Modulation of M current in SCG neurons by $[Ca^{2+}]_i$. (A) SCG neurons were cultured for 48–72 h and simultaneous recording of M current and monitoring of $[Ca^{2+}]_i$ performed. Fura-2 (100 μM) was loaded into the cells via the patch pipette. Plotted are the amplitudes of the deactivating time-dependent relaxations at −60 mV from pulses given every 3 s (black circles), and $[Ca^{2+}]_i$ (red line), calculated from the fura-2 emission. Measurement was started in EGTA-buffered Ca^{2+}-free solution, and solutions containing 2 mM Ca^{2+} plus 5 μM ionomycin or the M-current blocker linopirdine (LP, 50 μM) were applied during the periods indicated by the bars. The bottom panel shows representative current traces at the indicated times during the experiment. (B) Correlation of changes in $[Ca^{2+}]_i$ (hatched columns) and M current amplitude (solid columns) induced by the application of the 2 Ca ionomycin solution (n = 9). ***, significance at the P ≤ 0.001 level, paired Student's t test.

2002). Thus, we extended such experiments to the other subtypes. To probe for CaM interactions with KCNQ2–5, we performed immunoprecipitation (IP) experiments, followed by immunoblotting. KCNQ2–5 subunits were epitope tagged by introduction of the myc epitope to their amino termini and individually expressed in CHO cells. Current properties of KCNQ2–5 channels were not affected by introduction of the myc epitope (unpublished data). In immunoblots prepared from whole-cell lysates of CHO cells individually transfected with myc-tagged KCNQ2–5 channels, anti-myc antibodies specifically labeled the channels at the molecular weights of ∼100 kD for KCNQ2, 110 kD for KCNQ3, 80 kD for KCNQ4, and 125 kD for KCNQ5 (Fig. 3 A, bottom). Lysate from cells expressed with wt KCNQ3 was not labeled, showing the specificity of the myc antibodies (unpublished data). CHO cells were individually transfected with myc-tagged KCNQ2–5, together with wt or DN CaM. IPs were performed using anti-CaM antibodies of whole-cell lysates, either in the presence of 5 mM Ca^{2+}, or of 5 mM EGTA. The immunoprecipitated proteins were run as Western gels and immunoblotted with anti-myc antibodies. The immunoblots strongly labeled myc-tagged KCNQ2–5 when expressed with either wt or DN CaM, and in both high or low $[Ca^{2+}]$-immunoprecipitating conditions (Fig. 3 A, top middle). Thus, there is an association of both wt and DN CaM with KCNQ2–5 channels at both high and low $[Ca^{2+}]_i$.

In separate experiments, we compared the ability of anti-CaM antibodies to IP myc–tagged KCNQ2 and KCNQ3 in lysates from cells cotransfected with wt CaM or cells only transfected with the channels. We also used an antibody against focal adhesion kinase (FAK) as an irrelevant antibody IP control. FAK is endogenously expressed in CHO cells, but is not expected to bind to KCNQ channels. Fig. 3 B shows that a faint signal was seen for KCNQ3, and a very faint signal was seen for KCNQ2 in lysates from cells not cotransfected with CaM (top panel). The signals were much stronger for both KCNQ2 and KCNQ3 in lysates from cells cotransfected with wt CaM (middle panel). When the anti-FAK antibody was used for IP instead of the anti-CaM antibody, there were no detectable signals at all (bottom panel). The faint signals from CHO cells not transfected with CaM implies that there must be some level of endogenous CaM expression in CHO cells since the anti-CaM antibody used for IP should only pull down CaM (and any CaM-associated proteins). We thus compared CaM expression in CHO cells transfected with wt CaM, with DN CaM, or with no CaM. Fig. 3 B (bottom) shows that cells not transfected with any CaM express a low, but detectable, level of endogenous CaM, and that transfection of wt or DN CaM strongly increases the CaM signal seen on immunoblot. The stronger signal for DN CaM versus wt CAM does not necessarily mean that DN CaM expresses better than wt CaM, since our antibody seems to recognize apoCaM better than Ca^{2+}-bound CaM (see Fig. 1, inset). The weak, but detectable, endogenous expression of CaM in CHO cells is consistent with the variable, but generally weak, sensitivity of KCNQ2/3 channels to $[Ca^{2+}]_i$ seen in cells not cotransfected with CaM. In the electrophysiology experiments, there would have to be enough endogenous CaM to partner with the expressed KCNQ2/3 channels for the channels to be

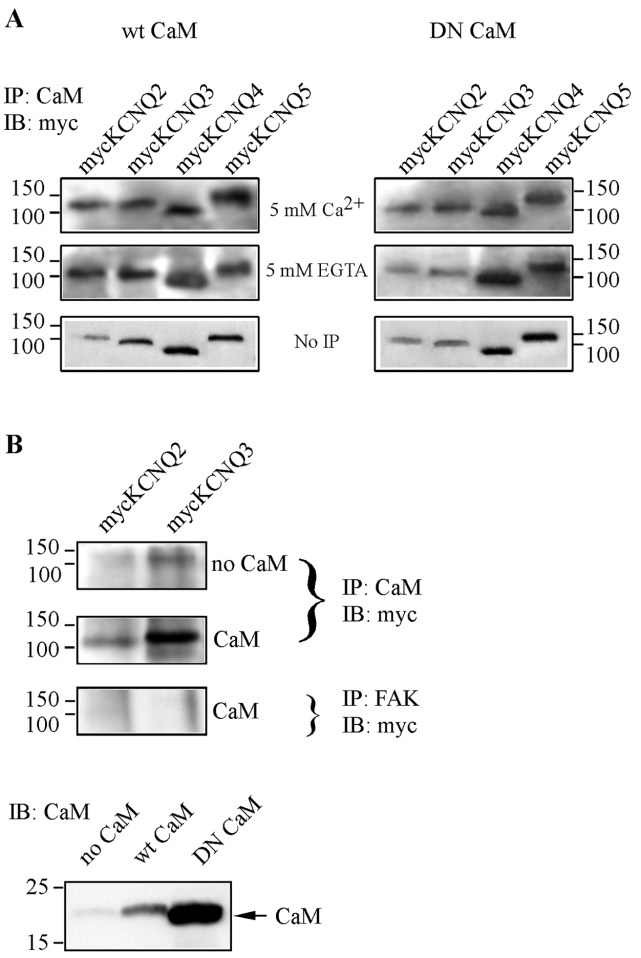

FIGURE 3. CaM coimmunoprecipitates with KCNQ2–5 channels. (A) CHO cells were transfected individually with myc-tagged KCNQ2–5 channels and either wt CaM or DN CaM, as indicated. Lysate proteins were immunoprecipitated in the presence of either 5 mM Ca^{2+} (top panels) or 5 mM EGTA (middle panels) with anti-CaM antibodies, the immunoprecipitates run as immunoblots and probed with anti-myc antibodies. The bottom panels show immunoblots using anti-myc antibodies from the same lysates as in the upper and middle panels, without immunoprecipitation. (B) CHO cells were transfected with myc-tagged KCNQ2 or KCNQ3 channels, either alone (top) or together with wt CaM (middle, lower). Lysate proteins were immunoprecipitated with either anti-CaM antibodies (top, middle), or anti-FAK antibodies (lower), the immunoprecipitates run as immunoblots and probed with anti-myc antibodies. The bottom panel is an immunoblot of lysates from CHO cells transfected with wt CaM, DN CaM, or no CaM, and probed with anti-CaM antibodies. We find that our anti-CaM antibodies have higher affinity for apoCaM than for Ca^{2+}-bound CaM.

mostly $[Ca^{2+}]_i$-sensitive, and the results in Fig. 1 and the immunoblot analysis here indicate that this is likely not the case. However, the highly sensitive IP assay requires only a low level of endogenous CaM to produce a weak IP signal in cells not cotransfected with CaM.

If CaM associates with KCNQ2–5 channels in the presence or absence of Ca^{2+}, where might it act to modulate the channels in a Ca^{2+}-dependent manner? Inspection of KCNQ2 and KCNQ3 channel sequences reveals two carboxy terminus domains that have similarity to the "IQ" domains originally described from CaM interactions with myosin domains of the general motif *I-Q-x-x-I-R/K-G-x-x-x-R/K* (Houdusse and Cohen, 1996). Subsequent work has revealed CaM to be the Ca^{2+} sensor for a number of different ion channels that are sensitive to $[Ca^{2+}]_i$ and that CaM often acts at such IQ domains on these channels to modulate them upon $[Ca^{2+}]_i$ rises. For several different channels modulated in this way, CaM acts by binding to IQ domains in a Ca^{2+}-dependent manner, although CaM may be pretethered to the channels in its Ca^{2+}-free "apoCaM" form (for review see Saimi and Kung, 2002). In the case of the more distal of the two IQ domains seen in KCNQ channels, its sequence also has features of the 1-5-10 type of CaM-binding domain (Rhoads and Friedberg, 1997; Yus-Najera et al., 2002). We focused on KCNQ2 and KCNQ3 and will call their two IQ-like domains IQ_1 and IQ_2 (Fig. 4 A).

To test for interactions between CaM and these putative CaM-binding domains, we performed gel-shift assays using purified recombinant CaM protein and synthesized peptides containing IQ_1 and IQ_2 of KCNQ2 and KCNQ3 (see MATERIALS AND METHODS). As a positive control, we also used a peptide from the IQ-like domain identified on the $Ca_V1.2$ (α_{1C}, L-type) Ca^{2+} channel that has been shown to directly bind CaM in a Ca^{2+}-dependent manner on gel-shift assays (IQ_L peptide) (Peterson et al., 1999). CaM protein was preincubated at different peptide/CaM molar ratios or just with peptide buffer, and the incubations run on nondenaturing (native) PAGE. The migrated proteins were visualized either by silver staining the gels, or by transferring the proteins to nitrocellulose and immunoblotting with anti-CaM antibodies. The gel-shift assays were run in the presence of either 2 mM Ca^{2+} or 2 mM EGTA in the sample and running buffers. We found that, in the presence of Ca^{2+}, inclusion of the IQ_2 peptides of both KCNQ2 and KCNQ3, or the IQ_L peptide, caused a shift in the mobility of CaM in the gel. However, for all three peptides, there was no shift in CaM mobility in the absence of Ca^{2+} (Fig. 4 B, $n = 3$). We did not observe a mobility shift when we performed this same test using any of the IQ_1 peptides of KCNQ2 and 3 at molar ratios up to 10:1 peptide:CaM. Thus, we suggest that the Ca^{2+}-dependent site of action on KCNQ2 and KCNQ3 subunits of Ca^{2+}/CaM may be at their IQ_2 domain.

Ca^{2+}/CaM Mediates Bradykinin Inhibition of Neuronal M Current

The data presented in Figs. 1–4 suggest that CaM can act as the Ca^{2+} sensor of cloned KCNQ2/3 channels, and of native M channels, and could mediate Ca^{2+}-depen-

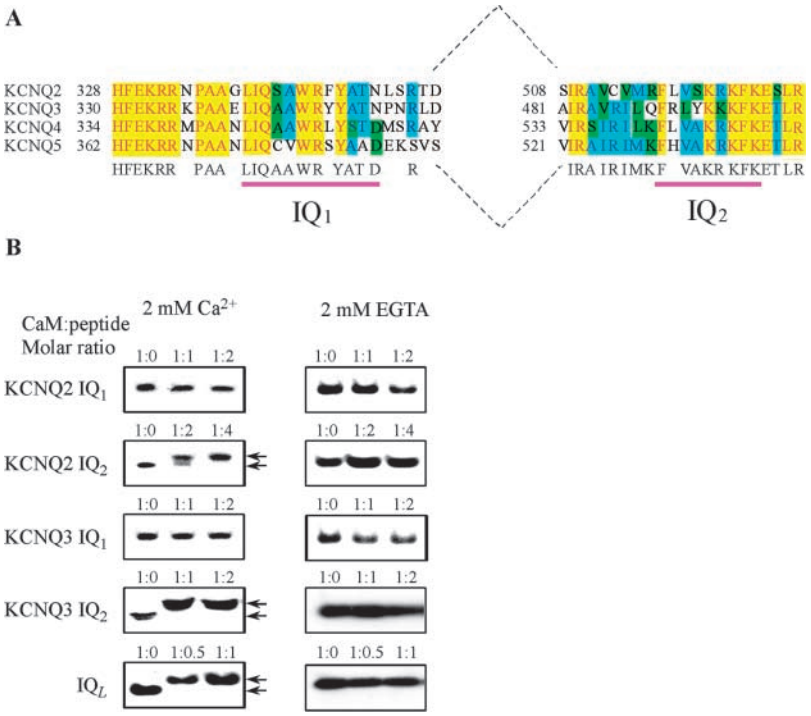

FIGURE 4. CaM interacts with an IQ-like domain in the carboxy terminus of KCNQ2 and KCNQ3. (A) Alignment of regions of KCNQ2–5 channels in the regions containing the IQ_1 and IQ_2 peptides tested in gel-shift assays. Below the alignment is the consensus sequence for residues with high similarity amongst KCNQ2–5. Yellow shading indicates completely conserved residues; green-shading indicates weakly conserved residues, and blue-shaded regions are consensus residues derived from a block of similar residues at a given position. The purple lines show the regions most "IQ-like" in these domains. (B) Gel shift assays. Shown are Comassie blue–labeled 15% nondenaturing Western gels of CaM incubated with IQ_1 and IQ_2 peptides of KCNQ2 (both KCNQ3 IQ_1 peptides given in MATERIALS AND METHODS gave the same negative result) and KCNQ3, and the IQ domain of the α_{1C} Ca^{2+} channel (IQ_L) in the presence of 2 mM Ca^{2+} (left) or of 2 mM EGTA (right) in the sample and running buffers at CaM/peptide molar ratios indicated above each lane. The double arrows point to the position of CaM either alone, or bound to peptide.

dent modulation. Since bradykinin suppression of M current in rat sympathetic neurons involves a rise in $[Ca^{2+}]_i$ and is blocked by agents that prevent such rises (Cruzblanca et al., 1998; Delmas et al., 2002), we hypothesized that CaM can act as the Ca^{2+} sensor of native M current as well and can be involved in bradykinin modulation. We tested such a role for CaM in bradykinin actions on M current in cultured rat superior cervical ganglion (SCG) sympathetic neurons by exogenous expression in the neurons of wt or DN CaM, using the Sinbis alphaviral method (Gamper et al., 2003; Straiker et al., 2002). WT or DN CaM was transduced into the neurons along with EGFP in the form of a bicistronic vector (see MATERIALS AND METHODS) that also contains EGFP, and green-fluorescing neurons were chosen for study. We found that neurons infected with pseudovirions the previous night appeared healthy and were suitable for patch-clamp study for most of the following day. The left inset in Fig. 5 shows transmitted light and fluorescent (λ_{exit} = 470 nm) micrographs of a successfully transduced SCG cell using the Sinbis method.

We compared the ability of bradykinin and the muscarinic receptor agonist oxotremorine (oxo-M) to inhibit SCG M current in the three groups of cells using whole-cell clamp. These experiments did not attempt to control $[Ca^{2+}]_i$ with our ionomycin-containing bath solutions, and used our usual pipette solution containing 100 μM BAPTA that allows $[Ca^{2+}]_i$ to change (Beech et al., 1991). We found that bradykinin inhibition was much smaller in cells transduced with wt CaM or with DN CaM, compared with those transduced only with EGFP, but muscarinic inhibition was unaffected (Fig. 5, A–C, left). Such data are summarized in Fig. 5 D (solid bars). For neurons transduced with EGFP only (control), inhibition by bradykinin (250 nM) was 74 ± 7% (n = 8); for those with DN CaM, it was 30 ± 9% (n = 10; $P \leq 0.001$), and for those with wt CaM, it was 33 ± 7% (n = 7; $P \leq 0.001$). However, inhibition of M current by oxo-M (10 μM) was similar in the three groups of cells, for which the inhibitions were 91 ± 1% (n = 8), 89 ± 2% (n = 10), and 75 ± 6% (n = 7), respectively.

Some investigators have reported subtle differences in M current physiology when recording currents in the perforated-patch versus whole-cell configuration. In addition, we wanted a control for any possible unanticipated effects of our psuedovirions used in the Sinbis expression system. Thus, as a second method of expression of exogenous genes in SCG neurons, we used the biolistic "gene gun" method (Malin and Nerbonne, 2000). As for the Sinbis experiments, cultured SCG neurons were transfected with the bicistronic vectors containing either wt CaM and EGFP, DN CaM and EGFP, or EGFP alone. Neurons were cultured overnight, "shot" with DNA-coated gold particles using the gene gun, and green-fluorescing neurons studied the following day. We did not see any deleterious effects of penetration by the gold particles. The right inset in Fig. 5 shows transmitted light (left) and fluorescent (right, λ_{exit} = 470 nm) micrographs of a successfully transfected SCG cell using the gene gun method.

We performed parallel experiments to those done us-

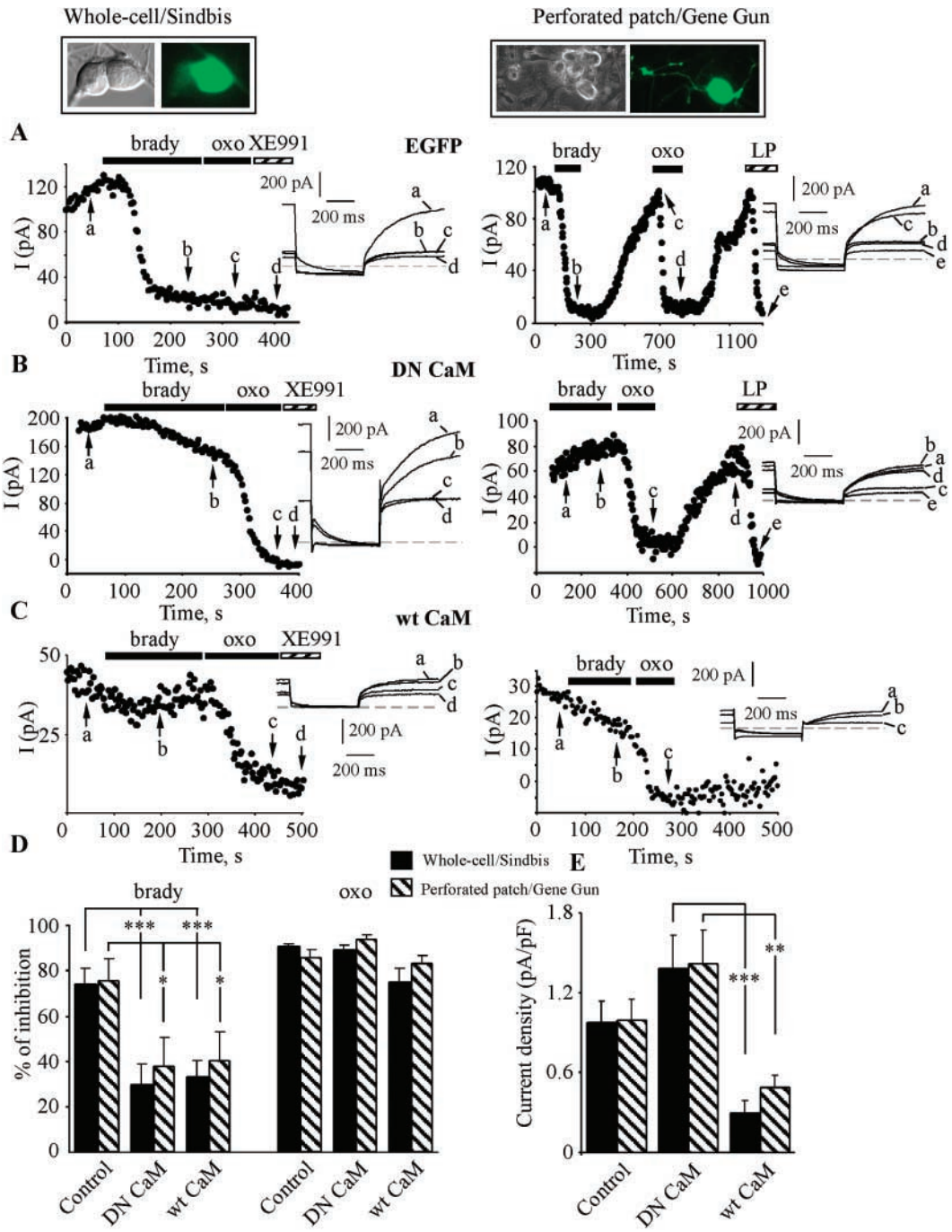

FIGURE 5. Bradykinin inhibition of SCG M current is mimicked or blocked by wt or DN CaM. M currents were recorded from cultured SCG neurons using the pulse protocol described in MATERIALS AND METHODS. (A–C) Plotted on the panels are the amplitudes of the deactivating time-dependent relaxations at −60 mV from pulses given every 3 s for neurons exogenously expressed with EGFP alone (A), or together with DN CaM (B) or wt CaM (C) using two different expression methods and recording techniques. On the left are shown experiments using the *Sinbis* expression system and whole-cell recording, and on the right are shown experiments using the biolistic "gene gun" and perforated-patch recording (MATERIALS AND METHODS). Bradykinin (250 nM), oxo-M (10 μM), XE991 (50 μM), or linopirdine (LP, 50 μM) were bath applied during the periods shown by the bars. Shown on the right of the panels are representative current traces at the indicated times from these experiments. In the inset are shown brightfield (left) or fluorescent (right) images of two SCG neurons transduced with the Sinbis method (left), or transfected with the gene gun method (right). A neuron in each case displays EGFP fluorescence, indicating successful transduction/transfection and were typical of those chosen for study. (D) Bars show mean inhibitions by bradykinin or oxo-M for cells transduced/transfected with EGFP alone (Control), or together with DN CaM or wt CaM. The solid bars summarize the Sinbis/whole-cell experiments and the hatched bars the gene gun/perforated-patch experiments. (E) Bars show mean initial M current density measured at −60 mV, normalized as pA/pF, for neurons transduced/transfected with EGFP only (Control), or together with DN CaM or wt CaM. ***, significance at the $P \leq 0.001$; **, $P \leq 0.01$; *, or $P \leq 0.05$ levels, Student's *t* test.

ing Sinbis transduction and whole-cell recording on SCG cells transfected with the gene gun, using perforated-patch recording. We again compared the ability of bradykinin and oxo-M to inhibit SCG M current in the three groups of cells. As before, we found that bradykinin inhibition was much smaller in cells transfected with wt CaM or with DN CaM, compared with those transfected only with EGFP, but muscarinic inhibition was unaffected (Fig. 5, A–C, right). Such data are summarized in Fig. 5 D (hatched bars). For neurons transfected with EGFP only (control), inhibition by bradykinin (250 nM) was 76 ± 9% (n = 7); for those with DN CaM, it was 38 ± 12% (n = 7; P ≤ 0.05), and for those with wt CaM, it was 40 ± 13% (n = 6; P ≤ 0.05). However, inhibition of M current by oxo-M (10 μM) was similar in the three groups of cells, for which the inhibitions were 86 ± 4% (n = 6), 94 ± 2% (n = 6), and 83 ± 4% (n = 5), respectively. Thus, experiments on SCG neurons transduced with Sinbis pseudovirions, or transfected with the gene gun, and studied using the whole-cell or perforated-patch recording techniques give the same result. Expression of wt or DN CaM greatly affects bradykinin modulation, but has no effect on modulation by muscarinic agonists.

One interpretation of the reduced inhibition by bradykinin in both DN CaM and wt CaM cells is that in the former, bradykinin action is blocked by DN CaM, which competes with endogenous CaM and prevents Ca^{2+}-mediated modulation; whereas, in the latter, overexpression of wt CaM increases tonic Ca^{2+} modulation, mimicking bradykinin-induced suppression of M current. In both cases, the extent of bradykinin modulation would be greatly reduced, but this hypothesis predicts that, as in the case in our CHO cell experiments, the initial M current density in SCG cells should be much reduced in cells transduced/transfected with wt CaM, and perhaps somewhat larger in cells transduced/transfected with DN CaM. Fig. 5 E summarizes our data showing that this was precisely the case, both for the Sinbis/whole-cell experiments and for the gene gun/perforated-patch experiments. For the Sinbis/whole-cell experiments, for SCG cells transduced only with EGFP, M current density (at −60 mV) was 0.98 ± 0.19 pA/pF (n = 8); for those transduced with DN CaM, it was 1.38 ± 0.31 pA/pF (n = 11), and for those transduced with wt CaM, it was reduced to 0.30 ± 0.04 pA/pF (n = 12, P ≤ 0.002). For the gene gun/perforated-patch experiments, for SCG cells transfected only with EGFP, M current density (at −60 mV) was 0.99 ± 0.16 pA/pF (n = 9); for those transfected with DN CaM, it was 1.42 ± 0.25 pA/pF (n = 8), and for those transfected with wt CaM, it was reduced to 0.49 ± 0.09 pA/pF (n = 8, P ≤ 0.01). M current amplitudes, and the effects of wt or DN CaM overexpression on them, were very similar between the two recording and expression methods. These data suggest that Ca^{2+}/CaM mediates bradykinin inhibition of M current in SCG neurons, and that, as in the reconstituted system, overexpression in the cells of DN CaM or wt CaM blocks, or amplifies, Ca^{2+}-mediated actions, respectively.

CaM Does Not Alter Bradykinin-induced Ca^{2+} Rises

We considered the possibilities that the effects of DN CaM or wt CaM on bradykinin modulation could be due to alterations in IP_3 production, or on downstream release of Ca^{2+} from intracellular stores. To rule out these possibilities, we investigated the extent of rises in $[Ca^{2+}]_i$ induced by bradykinin. $[Ca^{2+}]_i$ was monitored by bath-loading fura-2 into cultured SCG neurons as the AM ester and imaging of $[Ca^{2+}]_i$ in individual or small groups of cultured cells. To ensure that intracellular Ca^{2+} stores were well-loaded, we used a protocol that began with perfusion of cells in a high K^+ bath solution (30 mM), which sets the cell-resting potential in a range where there is sufficient influx of Ca^{2+} through voltage-gated Ca^{2+} channels to load stores. This method has been shown to facilitate release of $[Ca^{2+}]_i$ from stores by $G_{q/11}$-coupled receptors in SCG neurons (del Rio et al., 1999). We then assayed the ability of bradykinin (250 nM) to induce rises in $[Ca^{2+}]_i$ in neurons transduced only with EGFP using the Sinbis method, with DN CaM, or with wt CaM. We observed obvious bradykinin-induced rises in $[Ca^{2+}]_i$ in about two-thirds of the neurons in all three groups (9 of 13, 13 of 23, and 14 of 28 neurons, respectively). Typical

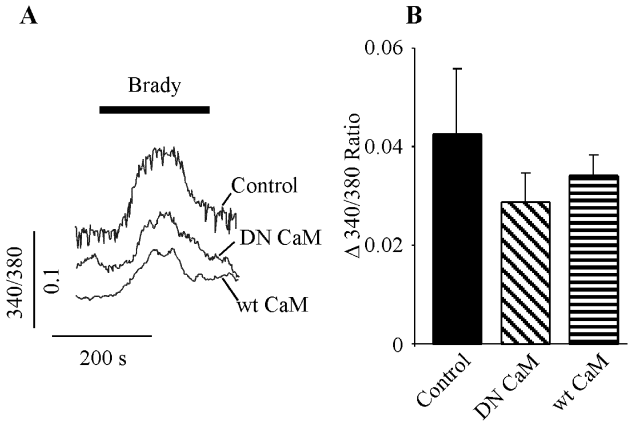

FIGURE 6. Bradykinin-induced Ca^{2+} rises in SCG neurons are not disturbed by wt or DN CaM. Shown in A are 340/380 nm ratiometric records of fura-2 emission from SCG cells transduced with EGFP only (Control) or together with wt CaM or DN CaM using the *Sinbis* method. Fura-2 was bath loaded into SCG neurons as the AM ester for 30 min before the experiment. A high K^+ bath solution (30 mM) was first applied (which raises $[Ca^{2+}]_i$ and loads stores) several minutes before application of bradykinin (250 nM). The traces have been offset from each other for clarity. We did not calibrate $[Ca^{2+}]_i$ in these experiments. (B) Bars show mean increases in the 340/380 nm ratio by bradykinin (n = 9, 13, and 14 for control, DN CaM, and wt CaM, respectively).

Ca^{2+} rises induced by bradykinin are shown in Fig. 6 A (left) for a cell from each group. There was no significant difference in the extent of rises in $[Ca^{2+}]_i$, quantified as the change in the 340/380 nm ratio. We did not calibrate $[Ca^{2+}]_i$ with these AM-loaded fura-2 experiments as this is notoriously unreliable (Zhou and Neher, 1993). These data are summarized in Fig. 6 B. For neurons transduced with EGFP alone, DN CaM, or wt CaM, bradykinin caused a change in the 340/380 nm ratio of 0.04 ± 0.01 (n = 9), 0.03 ± 0.01 (n = 13), and 0.03 ± 0.01 (n = 14), respectively. We conclude that the reductions in bradykinin modulation of M current in neurons transduced/transfected with wt CaM or with DN CaM were not due to a diminished ability of bradykinin to release Ca^{2+} from stores in those cells and are indeed likely due to the role of CaM in Ca^{2+} modulation of the channels.

DISCUSSION

This work implicates CaM in modulation of M-type K^+ channels by intracellular Ca^{2+} and suggests that bradykinin modulation of M current in sympathetic neurons uses CaM in concert with rises of $[Ca^{2+}]_i$. In our reconstituted system using CHO cells, KCNQ2/3 channels expressed alone, without CaM, showed a weak and variable sensitivity to changes in $[Ca^{2+}]_i$. Cells coexpressed with a DN CaM that cannot bind Ca^{2+} displayed KCNQ2/3 currents with almost no sensitivity to $[Ca^{2+}]_i$ over a physiological range from <10 nM to 400 nM. However, those coexpressed with wt CaM as well as KCNQ2/3 channels displayed currents that were highly Ca^{2+} sensitive over this range. Similar to KCNQ2/3 current in CHO cells overexpressing wt CaM, native M current in SCG neurons was also found to be highly Ca^{2+} sensitive. Gel-shift assays suggest that the site of CaM action on KCNQ2 and 3 subunits may be at a domain sharing features of IQ and 1-5-10 domains identified on other Ca^{2+}-sensitive channels. Finally, bradykinin modulation of native M current, which involves rises in $[Ca^{2+}]_i$, is blocked by expression in the neurons of DN CaM and mimicked by expression of wt CaM. Thus, we suggest that CaM acts as a Ca^{2+} sensor of M-type channels, endowing them with a high sensitivity to changes in $[Ca^{2+}]_i$.

Previous work on the action of $[Ca^{2+}]_i$ on M current has revealed differences in the $[Ca^{2+}]_i$ sensitivity of mammalian and amphibian M currents. Whereas M channels in rat SCG neurons were suggested to be highly Ca^{2+} sensitive, with rises of $[Ca^{2+}]_i$ depressing channel activity (Selyanko and Brown, 1996a,b), M current in frog sympathetic neurons seems to have a more complex Ca^{2+} sensitivity. It has been shown that increases of $[Ca^{2+}]_i$ in the range of 60–120 nM augments M current in such neurons whereas further rises above 200 nM have an inhibitory effect (Marrion et al., 1991; Yu et al., 1994; Marrion, 1996). In addition, calcineurin involvement has been suggested in the frog (Marrion, 1996), but ruled out in the rat (Selyanko and Brown, 1996a). Perhaps the mechanisms conferring Ca^{2+} sensitivity of M current in lower vertebrates differs from those of mammalian cells.

Since this work focuses on M channels in mammalian cells, of most relevance to this study is the work of Alex Selyanko in David Brown's lab (Selyanko and Brown, 1996a,b). Using inside-out patches from SCG neurons, they found an "exquisite" sensitivity of single M channels to cytoplasmic-facing $[Ca^{2+}]_i$, with an EC_{50} of ~100 nM and maximal inhibition of 87%. Interestingly, they found that not all patches from SCG cells had Ca^{2+} sensitivity to their M channels (28 of 44 patches) and speculated that perhaps a Ca^{2+}-sensing auxiliary protein sometimes dissociated away. Our results with KCNQ2/3 channels are quantitatively congruent with theirs and suggest that the needed auxiliary protein was calmodulin. The similarity of the concentration dependence of Ca^{2+} actions reported here (IC_{50} = 70 nM) and that of Selyanko and Brown (1996a) imply that our global measurements of $[Ca^{2+}]_i$ in CHO cells are a reasonable indicator of Ca^{2+} sensed by KCNQ2/3 channels. Although the extent of bradykinin-induced rises of $[Ca^{2+}]_i$ are modest (this study; Cruzblanca et al., 1998; Delmas et al., 2002), we found that when partnered with CaM, KCNQ2/3 channels are indeed exquisitely sensitive to $[Ca^{2+}]_i$ right in the range measured for resting $[Ca^{2+}]_i$ in sympathetic neurons. Furthermore, the steepness of the Ca^{2+} dependence that we observed means that bradykinin-induced rises of $[Ca^{2+}]_i$ within 100 nM in amplitude would be more than sufficient to have a large effect on M current.

A more subtle permissive effect of intracellular Ca^{2+} on muscarinic modulation has been described that arises from the blocking action of intracellular Ca^{2+} buffers on mAchR inhibition of M-type K^+ and N-type Ca^{2+} channels (Beech et al., 1991; Shapiro et al., 1994, 2000; Cruzblanca et al., 1998). In the present work, muscarinic inhibition of M current in SCG cells transduced with DN CaM was unaffected in the same cells in which bradykinin inhibition was strongly blocked. Thus, it seems unlikely that CaM mediates this permissive effect of $[Ca^{2+}]_i$ on muscarinic modulation of M current. Probably another Ca^{2+}-binding protein (Burgoyne and Weiss, 2001; Guo et al., 2002) is involved in this action or the site of this Ca^{2+} action is not within the channel, but within some other protein, e.g., phospholipase C (Suh and Hille, 2002).

Much recent work has highlighted the role of CaM in mediating Ca^{2+} regulation of a number of different ion channels. Although binding of Ca^{2+} to CaM is the switch in all of these actions, subtle differences have been found in the precise mechanism by which Ca^{2+}/

CaM works. A central variant is whether calmodulin is a dissociable or constitutive partner of the targeted channels. Examples of the former type of CaM/channel modulation are the cyclic nucleotide–gated (Chen and Yau, 1994; Hsu and Molday, 1994; Varnum and Zagotta, 1997; Trudeau and Zagotta, 2002), EAG K^+ (Schonherr et al., 2000), and NMDA channels (Ehlers et al., 1996). Examples of the latter type of action (often called the "pretethering mechanism") are the SK K^+ and L-type Ca^{2+} channels (for reviews see Levitan, 1999; Saimi and Kung, 2002). Even in the latter two cases, true pretethering of Ca^{2+}-free apoCaM has been difficult to unequivocally show, although the method of 3-cube FRET has proven powerful in this regard (Erickson et al., 2001).

Two recent papers have reported on the biochemistry of calmodulin binding to KCNQ channels (Wen and Levitan, 2002; Yus-Najera et al., 2002). Using similar biochemical approaches, both papers demonstrated CaM binding to the intracellular COOH-terminal domains of KCNQ2 and KCNQ3 channels, and disruption of binding by mutagenesis of residues at regions similar to those named IQ_1 and IQ_2 in the present study. The former work suggested that CaM is not involved in Ca^{2+} modulation of M-type channels, but rather in their assembly in the membrane, a secondary role for CaM also suggested for SK4/IK1 K^+ channels (Joiner et al., 2001). While we did not systematically investigate this issue, we did not observe less KCNQ2/3 current in cells not cotransfected with wt CaM or in those cotransfected with DN CaM. Rather, we found that currents were smaller in cells overexpressing CaM and greater in cells overexpressing DN CaM, which is more consistent with a role for CaM in Ca^{2+} sensing than in channel assembly. It may be, however, that CaM has a dual role in KCNQ channel physiology.

As in the present work, both Yus-Najera et al. (2002) and Wen and Levitan (2002) found both Ca^{2+}-dependent and -independent aspects of CaM–KCNQ channel interactions. The first group suggest a Ca^{2+} dependence of the interaction that is inverted: CaM binds to the channels better in the absence of Ca^{2+} and tends to dissociate upon $[Ca^{2+}]_i$ rise, and DN CaM was found not to interact with the channels. The second group found that both wt CaM and DN CaM interact with KCNQ2, consistent with our results that DN CaM can act as a dominant negative in CaM actions. Both groups report that mutations in regions containing our IQ_1 and IQ_2 sequences disrupted CaM–channel interactions. Given the importance that both groups ascribed to both of these regions for CaM binding to KCNQ2 subunits, we were surprised to find in the current work that IQ_2, but not IQ_1, produced a Ca^{2+}-dependent gel shift of CaM. Interestingly, our IQ_2 domains also contain the 1-5-10 type of CaM-binding motif like that used by NMDA channels to bind to CaM in a nonconstitutive way (Ehlers et al., 1996), perhaps intriguingly predicting our results for KCNQ2/3 heteromultimers that seem to fit to neither a strict pretethering nor dissociable model.

The effects of overexpression of wt CaM in reducing basal KCNQ2/3 currents in CHO cells or M current in SCG neurons suggest that at resting $[Ca^{2+}]_i$, a significant fraction of the channels may be CaM free. We suggest that overexpression of wt CaM creates more Ca^{2+}-bound CaM molecules able to interact with the channels, thus increasing tonic CaM action. At resting $[Ca^{2+}]_i$ (~60 nM) in our CHO cells coexpressing wt CaM, some fraction of channels are tonically modulated. We were then able to alter the modulation by externally varying $[Ca^{2+}]_i$, increasing or decreasing the current. In SCG cells, the resting $[Ca^{2+}]_i$ has been measured to be in the 50–100 nM range (Thayer et al., 1988; Beech et al., 1991; Trouslard et al., 1993; Cruzblanca et al., 1998; del Rio et al., 1999; Delmas et al., 2002) and so by overexpressing wt CaM, we likewise reason that many more M-channels than usual are tonically modulated by Ca^{2+}/CaM before bradykinin stimulation. Our ionomycin experiments in SCG cells (Fig. 2) confirm the tonic Ca^{2+} modulation of M channels suggested by previous work (Selyanko and Brown, 1996b). The disrupting abilities of DN CaM on Ca^{2+} modulation of KCNQ2/3 channels in CHO cells and on bradykinin modulation of M current in SCG cells strongly imply that DN CaM can interact with the channels.

While there are several models that might explain our results, we find attractive one that involves a generally modest affinity of apoCaM for the channels, with a higher affinity for them of Ca^{2+}/CaM, and consequently a distinct and strong affinity of Ca^{2+} for the CaM–channel complex. This idea is supported by the observations that the affinity of Ca^{2+} for apoCaM, which is usually in the low μM range, is often increased a thousand-fold upon binding of apoCaM to its substrate, and that the affinity of apoCaM for IQ-like domains can be quite variable, depending on the exact sequence involved (Jurado et al., 1999). Thus, overexpression of wt CaM leads to greater association of the channels with CaM by mass action and to their greater tonic inhibition at resting Ca^{2+}. Overexpression of DN CaM, however, leads to greater association of the channels with DN CaM over endogenous CaM, resulting in channels that remain Ca^{2+}-insensitive and in SCG M current that is not modulated by bradykinin. Future work will seek to determine the affinity and kinetics of the binding of apoCaM and Ca^{2+}/CaM to KCNQ channels and for the binding of Ca^{2+} to the CaM–channel binding domain complexes. Such experiments will determine the precise model of CaM action, and yield in-

sights into the physiological responses that couple changes in Ca^{2+} to control of M current, and thus, to regulation of neuronal excitability.

We thank Pamela Martin, Emily McDermott and Christy Glasow for expert technical assistance, James D. Stockand and Rachel E. Booth for many helpful discussions, and Nancy Markum for expert clerical support.

This work was supported by National Institutes of Health grant R01 NS43394 and by a Howard Hughes Medical Institute New Faculty Startup grant to MSS.

Olaf S. Andersen served as editor.

Submitted: 31 December 2002
Revised: 28 April 2003
Accepted: 13 May 2003

REFERENCES

Beech, D.J., L. Bernheim, A. Mathie, and B. Hille. 1991. Intracellular Ca^{2+} buffers disrupt muscarinic suppression of Ca^{2+} current and M current in rat sympathetic neurons. *Proc. Natl. Acad. Sci. USA.* 88:652–656.

Bernheim, L., D.J. Beech, and B. Hille. 1991. A diffusible second messenger mediates one of the pathways coupling receptors to calcium channels in rat sympathetic neurons. *Neuron.* 6:859–867.

Bernheim, L., A. Mathie, and B. Hille. 1992. Characterization of muscarinic receptor subtypes inhibiting Ca^{2+} current and M current in rat sympathetic neurons. *Proc. Natl. Acad. Sci. USA.* 89: 9544–9548.

Bofill-Cardona, E., N. Vartian, C. Nanoff, M. Freissmuth, and S. Boehm. 2000. Two different signaling mechanisms involved in the excitation of rat sympathetic neurons by uridine nucleotides. *Mol. Pharmacol.* 57:1165–1172.

Brown, D.A., and P.R. Adams. 1980. Muscarinic suppression of a novel voltage-sensitive K^+ current in a vertebrate neurone. *Nature.* 283:673–676.

Burgoyne, R.D., and J.L. Weiss. 2001. The neuronal calcium sensor family of Ca^{2+}-binding proteins. *Biochem. J.* 353:1–12.

Chen, T.Y., and K.W. Yau. 1994. Direct modulation by Ca^{2+}-calmodulin of cyclic nucleotide-activated channel of rat olfactory receptor neurons. *Nature.* 368:545–548.

Constanti, A., and D.A. Brown. 1981. M-Currents in voltage-clamped mammalian sympathetic neurones. *Neurosci. Lett.* 24: 289–294.

Cruzblanca, H., D.S. Koh, and B. Hille. 1998. Bradykinin inhibits M current via phospholipase C and Ca^{2+} release from IP_3-sensitive Ca^{2+} stores in rat sympathetic neurons. *Proc. Natl. Acad. Sci. USA.* 95:7151–7156.

del Rio, E., J.A. Bevilacqua, S.J. Marsh, P. Halley, and M.P. Caulfield. 1999. Muscarinic M_1 receptors activate phosphoinositide turnover and Ca^{2+} mobilisation in rat sympathetic neurones, but this signaling pathway does not mediate M-current inhibition. *J. Physiol.* 520:101–111.

Delmas, P., D.A. Brown, M. Dayrell, F.C. Abogadie, M.P. Caulfield, and N.J. Buckley. 1998. On the role of endogenous G-protein beta gamma subunits in N-type Ca^{2+} current inhibition by neurotransmitters in rat sympathetic neurones. *J. Physiol.* 506:319–329.

Delmas, P., N. Wanaverbecq, F.C. Abogadie, M. Mistry, and D.A. Brown. 2002. Signaling microdomains define the specificity of receptor-mediated IP_3 pathways in neurons. *Neuron.* 34:209–220.

Ehlers, M.D., S. Zhang, J.P. Bernhadt, and R.L. Huganir. 1996. Inactivation of NMDA receptors by direct interaction of calmodulin with the NR1 subunit. *Cell.* 84:745–755.

Erickson, M.G., B.A. Alseikhan, B.Z. Peterson, and D.T. Yue. 2001. Preassociation of calmodulin with voltage-gated Ca^{2+} channels revealed by FRET in single living cells. *Neuron.* 31:973–985.

Gamper, N., J.D. Stockand, and M.S. Shapiro. 2003. Subunit-specific modulation of KCNQ potassium channels by Src tyrosine kinase. *J. Neurosci.* 23:84–95.

Geiser, J.R., D. van Tuinen, S.E. Brockerhoff, M.M. Neff, and T.N. Davis. 1991. Can calmodulin function without binding calcium? *Cell.* 65:949–959.

Grynkiewicz, G., M. Poenie, and R.Y. Tsien. 1985. A new generation of Ca^{2+} indicators with greatly improved fluorescence properties. *J. Biol. Chem.* 260:3440–3450.

Guo, W., S.A. Malin, D.C. Johns, A. Jeromin, and J.M. Nerbonne. 2002. Modulation of Kv4-encoded K^+ currents in the mammalian myocardium by neuronal calcium sensor-1. *J. Biol. Chem.* 277: 26436–26443.

Haeseleer, F., Y. Imanishi, I. Sokal, S. Filipek, and K. Palczewski. 2002. Calcium-binding proteins: intracellular sensors from the calmodulin superfamily. *Biochem. Biophys. Res. Commun.* 290:615–623.

Haley, J.E., F.C. Abogadie, P. Delmas, M. Dayrell, Y. Vallis, G. Milligan, M.P. Caulfield, D.A. Brown, and N.J. Buckley. 1998. The alpha subunit of G_q contributes to muscarinic inhibition of the M-type potassium current in sympathetic neurons. *J. Neurosci.* 18: 4521–4531.

Hamilton, S.E., M.D. Loose, M. Qi, A.I. Levey, B. Hille, G.S. McKnight, R.L. Idzerda, and N.M. Nathanson. 1997. Disruption of the m1 receptor gene ablates muscarinic receptor-dependent M current regulation and seizure activity in mice. *Proc. Natl. Acad. Sci. USA.* 94:13311–13316.

Houdusse, A., and C. Cohen. 1996. Structure of the regulatory domain of scallop myosin at 2 A resolution: implications for regulation. *Structure.* 4:21–32.

Hsu, Y.T., and R.S. Molday. 1994. Interaction of calmodulin with the cyclic GMP-gated channel of rod photoreceptor cells. Modulation of activity, affinity purification, and localization. *J. Biol. Chem.* 269:29765–29770.

Jentsch, T.J. 2000. Neuronal KCNQ potassium channels: physiology and role in disease. *Nat. Rev. Neurosci.* 1:21–30.

Joiner, W.J., R. Khanna, L.C. Schlichter, and L.K. Kaczmarek. 2001. Calmodulin regulates assembly and trafficking of SK4/IK1 Ca^{2+}-activated K^+ channels. *J. Biol. Chem.* 276:37980–37985.

Jones, S., D.A. Brown, G. Milligan, E. Willer, N.J. Buckley, and M.P. Caulfield. 1995. Bradykinin excites rat sympathetic neurons by inhibition of M current through a mechanism involving B_2 receptors and $G_{\alpha q/11}$. *Neuron.* 14:399–405.

Jurado, L.A., P.S. Chockalingam, and H.W. Jarrett. 1999. Apocalmodulin. *Physiol. Rev.* 79:661–682.

Keen, J.E., R. Khawaled, D.L. Farrens, T. Neelands, A. Rivard, C.T. Bond, A. Janowsky, B. Fakler, J.P. Adelman, and J. Maylie. 1999. Domains responsible for constitutive and Ca^{2+}-dependent interactions between calmodulin and small conductance Ca^{2+}-activated potassium channels. *J. Neurosci.* 19:8830–8838.

Lee, A., S.T. Wong, D. Gallagher, B. Li, D.R. Storm, T. Scheuer, and W.A. Catterall. 1999. Ca^{2+}/calmodulin binds to and modulates P/Q-type calcium channels. *Nature.* 399:155–159.

Lerche, C., C.R. Scherer, G. Seebohm, C. Derst, A.D. Wei, A.E. Busch, and K. Steinmeyer. 2000. Molecular cloning and functional expression of KCNQ5, a potassium channel subunit that may contribute to neuronal M-current diversity. *J. Biol. Chem.* 275: 22395–22400.

Levitan, I.B. 1999. It is calmodulin after all! Mediator of the calcium modulation of multiple ion channels. *Neuron.* 22:645–648.

Malin, S.A., and J.M. Nerbonne. 2000. Elimination of the fast transient in superior cervical ganglion neurons with expression of

KV4.2W362F: molecular dissection of I_A. *J. Neurosci.* 20:5191–5199.

Marrion, N.V., R.S. Zucker, S.J. Marsh, and P.R. Adams. 1991. Modulation of M-current by intracellular Ca^{2+}. *Neuron.* 6:533–545.

Marrion, N.V. 1996. Calcineurin regulates M channel modal gating in sympathetic neurons. *Neuron.* 16:163–173.

Persechini, A., D.K. Blumenthal, H.W. Jarrett, C.B. Klee, D.O. Hardy, and R.H. Kretsinger. 1989. The effects of deletions in the central helix of calmodulin on enzyme activation and peptide binding. *J. Biol. Chem.* 264:8052–8058.

Peterson, B.Z., C.D. DeMaria, J.P. Adelman, and D.T. Yue. 1999. Calmodulin is the Ca^{2+} sensor for Ca^{2+}-dependent inactivation of L-type calcium channels. *Neuron.* 22:549–558.

Qin, N., R. Olcese, M. Bransby, T. Lin, and L. Birnbaumer. 1999. Ca^{2+}-induced inhibition of the cardiac Ca^{2+} channel depends on calmodulin. *Proc. Natl. Acad. Sci. USA.* 96:2435–2438.

Rae, J., K. Cooper, P. Gates, and M. Watsky. 1991. Low access resistance perforated patch recordings using amphotericin B. *J. Neurosci. Methods.* 37:15–26.

Rhoads, A.R., and F. Friedberg. 1997. Sequence motifs for calmodulin recognition. *FASEB J.* 11:331–340.

Roche, J.P., R. Westenbroek, A.J. Sorom, B. Hille, K. Mackie, and M.S. Shapiro. 2002. Antibodies and a cysteine-modifying reagent show correspondence of M current in neurons to KCNQ2 and KCNQ3 K^+ channels. *Br. J. Pharmacol.* 137:1173–1186.

Saimi, Y., and C. Kung. 2002. Calmodulin as an ion channel subunit. *Annu. Rev. Physiol.* 64:289–311.

Scholze, T., E. Moskvina, M. Mayer, H. Just, H. Kubista, and S. Boehm. 2002. Sympathoexcitation by bradykinin involves Ca^{2+}-independent protein kinase C. *J. Neurosci.* 22:5823–5832.

Schonherr, R., K. Lober, and S.H. Heinemann. 2000. Inhibition of human ether a go-go potassium channels by Ca^{2+}/calmodulin. *EMBO J.* 19:3263–3271.

Schroeder, B.C., M. Hechenberger, F. Weinreich, C. Kubisch, and T.J. Jentsch. 2000. KCNQ5, a novel potassium channel broadly expressed in brain, mediates M-type currents. *J. Biol. Chem.* 275: 24089–24095.

Selyanko, A.A., C.E. Stansfeld, and D.A. Brown. 1992. Closure of potassium M-channels by muscarinic acetylcholine-receptor stimulants requires a diffusible messenger. *Proc. R. Soc. Lond. B Biol. Sci.* 250:119–125.

Selyanko, A.A., and D.A. Brown. 1996a. Intracellular calcium directly inhibits potassium M channels in excised membrane patches from rat sympathetic neurons. *Neuron.* 16:151–162.

Selyanko, A.A., and D.A. Brown. 1996b. Regulation of M-type potassium channels in mammalian sympathetic neurons: action of intracellular calcium on single channel currents. *Neuropharmacology.* 35:933–947.

Selyanko, A.A., J.K. Hadley, I.C. Wood, F.C. Abogadie, T.J. Jentsch, and D.A. Brown. 2000. Inhibition of KCNQ1-4 potassium channels expressed in mammalian cells via M1 muscarinic acetylcholine receptors. *J. Physiol.* 522:349–355.

Shah, M.M., M. Mistry, S.J. Marsh, D.A. Brown, and P. Delmas. 2002. Molecular correlates of the M-current in cultured rat hippocampal neurons. *J. Physiol.* 544:29–37.

Shapiro, M.S., L.P. Wollmuth, and B. Hille. 1994. Angiotensin II inhibits calcium and M current channels in rat sympathetic neurons via G proteins. *Neuron.* 12:1319–1329.

Shapiro, M.S., J.P. Roche, E.J. Kaftan, H. Cruzblanca, K. Mackie, and B. Hille. 2000. Reconstitution of muscarinic modulation of the KCNQ2/KCNQ3 K^+ channels that underlie the neuronal M current. *J. Neurosci.* 20:1710–1721.

Straiker, A.J., C.R. Borden, and J.M. Sullivan. 2002. G-protein alpha subunit isoforms couple differentially to receptors that mediate presynaptic inhibition at rat hippocampal synapses. *J. Neurosci.* 22:2460–2468.

Suh, B., and B. Hille. 2002. Recovery from muscarinic modulation of M current channels requires phosphatidylinositol 4,5-bisphosphate synthesis. *Neuron.* 35:507–520.

Thayer, S.A., L.D. Hirning, and R.J. Miller. 1988. The role of caffeine-sensitive calcium stores in the regulation of the intracellular free calcium concentration in rat sympathetic neurons in vitro. *Mol. Pharmacol.* 34:664–673.

Tokimasa, T. 1996. Calcium-dependent after-hyperpolarization in dissociated bullfrog sympathetic neurons. *Neurosci. Lett.* 218:49–52.

Tokimasa, T., T. Shirasaki, M. Yoshida, M. Ito, E. Tanaka, T. Mitsumoto, T. Akasu, M. Tanaka, H. Higashi, and T. Nakano. 1996. Calcium-dependent potentiation of M-current in bullfrog sympathetic neurons. *Neurosci. Lett.* 214:79–82.

Tokimasa, T., T. Shirasaki, and K. Kuba. 1997. Evidence for the calcium-dependent potentiation of M-current obtained by the ratiometric measurement of the fura-2 fluorescence in bullfrog sympathetic neurons. *Neurosci. Lett.* 236:123–126.

Trouslard, J., S.J. Marsh, and D.A. Brown. 1993. Calcium entry through nicotinic receptor channels and calcium channels in cultured rat superior cervical ganglion cells. *J. Physiol.* 468:53–71.

Trudeau, M.C., and W.N. Zagotta. 2002. Mechanism of calcium/calmodulin inhibition of rod cyclic nucleotide-gated channels. *Proc. Natl. Acad. Sci. USA.* 99:8424–8429.

Varnum, M.D., and W.N. Zagotta. 1997. Interdomain interactions underlying activation of cyclic nucleotide-gated channels. *Science.* 278:110–113.

Wang, H.S., and D. McKinnon. 1995. Potassium currents in rat prevertebral and paravertebral sympathetic neurones: control of firing properties. *J. Physiol.* 485:319–335.

Wang, H.S., Z. Pan, W. Shi, B.S. Brown, R.S. Wymore, I.S. Cohen, J.E. Dixon, and D. McKinnon. 1998. KCNQ2 and KCNQ3 potassium channel subunits: molecular correlates of the M-channel. *Science.* 282:1890–1893.

Wen, H., and I.B. Levitan. 2002. Calmodulin is an auxiliary subunit of KCNQ2/3 potassium channels. *J. Neurosci.* 22:7991–8001.

Xia, X.M., B. Fakler, A. Rivard, G. Wayman, T. Johnson-Pais, J.E. Keen, T. Ishii, B. Hirschberg, C.T. Bond, S. Lutsenko, et al. 1998. Mechanism of calcium gating in small-conductance calcium-activated potassium channels. *Nature.* 395:503–507.

Yu, S.P., D.M. O'Malley, and P.R. Adams. 1994. Regulation of M current by intracellular calcium in bullfrog sympathetic ganglion neurons. *J. Neurosci.* 14:3487–3499.

Yus-Najera, E., I. Santana-Castro, and A. Villarroel. 2002. The identification and characterization of a non-continuous calmodulin binding site in non-inactivating voltage-dependent KCNQ potassium channels. *J. Biol. Chem.* 277:28545–28553.

Zaczek, R., R.J. Chorvat, J.A. Saye, M.E. Pierdomenico, C.M. Maciag, A.R. Logue, B.N. Fisher, D.H. Rominger, and R.A. Earl. 1998. Two new potent neurotransmitter release enhancers, 10,10-bis(4-pyridinylmethyl)-9(10H)-anthracenone and 10,10-bis (2-fluoro-4-pyridinylmethyl)-9(10H)-anthracenone: comparison to linopirdine. *J. Pharmacol. Exp. Ther.* 285:724–730.

Zhang, H., L.C. Craciun, T. Mirshahi, T. Rohacs, C.M. Lopes, T. Jin, and D.E. Logothetis. 2003. PIP_2 activates KCNQ channels, and its hydrolysis underlies receptor-mediated inhibition of M currents. *Neuron.* 37:963–975.

Zhou, Z., and E. Neher. 1993. Mobile and immobile calcium buffers in bovine adrenal chromaffin cells. *J. Physiol.* 469:245–273.

Zuhlke, R.D., G.S. Pitt, K. Deisseroth, R.W. Tsien, and H. Reuter. 1999. Calmodulin supports both inactivation and facilitation of L-type calcium channels. *Nature.* 399:159–162.